Revival-collapse phenomenon in the quadrature squeezing of the multiphoton intensity-dependent Jaynes-Cummings model

Faisal A. A. El-Orany[1]

[1] *Department of Mathematics and Computer Science, Faculty of Science, Suez Canal University, Ismailia, Egypt*

(Dated: September 2, 2009)

For multiphoton intensity-dependent Jaynes-Cummings model (JCM), which is described by two-level atom interacting with a radiation field, we prove that there is a relationship between the atomic inversion and the quadrature squeezing. We give the required condition to obtain best information from this relation. Also we show that this relation is only sensitive to large values of the detuning parameter. Furthermore, we discuss briefly such relation for the off-resonance standard JCM.

PACS numbers: 42.50.Dv, 32.80.-t, 42.50.-p.

arXiv:0909.0311v1 [quant-ph] 2 Sep 2009

I. INTRODUCTION

The interaction between the radiation field and matter (, i.e., atom), which is usually called Jaynes-Cummings model (JCM) [1], is one of the basic systems in quantum optics. The JCM system has become experimentally realizable with the Rydberg atoms in high-Q microwave cavities (, e.g., see [2]). Various extensions for JCM have been performed and investigated in greater details such as multiphoton [3], intensity-dependent [4], multimode, e.g., [5, 6, 7], multilevel atoms [8] and multiatom interactions [9]. In the framework of rotating-wave approximation the JCM has been exactly solved and many interesting features have been remarked, such as sub-Poissonian statistics [10], quadrature squeezing [11] and revival-collapse phenomenon (RCP) in the Rabi oscillation [12]. Furthermore, JCM has been used for generating nonclassical states via the conditional measurement technique [13]. As well known the most important phenomenon is the RCP in the evolution of the atomic inversion $\langle\hat{\sigma}_z(T)\rangle$ where both the collapse and the revival have quantum origins, the former is a less clear-cut quantum effect: the collapse appears even for the stochastic classical field, while the revival finds its origin in the granularity of the quantized radiation field. The revivals result from the beating of all nearest-neighbor Rabi oscillators and occur when the $\bar{n}$th and $(\bar{n}+1)$th oscillators become in phase [14]. Moreover, the envelope of each revival is readout of the photon distribution, in particular, for the states whose photon-number distributions are slowly varying [15]. For two-level atom in the excited (or ground) state interacting resonantly with the radiation

fields in coherent states with strong initial intensities–as far as we know–there are three different forms for the shape of the RCP based on the type of the Hamiltonian model: (i) For single-photon JCM [12] there is an initial collapse of these oscillations followed by regular revivals that slowly become broader and eventually overlap. In this case the revival pattern has a Gaussian shape. (ii) For two-photon JCM [16] and/or single-photon intensity-dependent JCM (IJCM) [4] the revival patterns are periodic (with period π), compact and systematic. (iii) For single-photon two-mode JCM the revival series is compact, each revival is followed by secondary revival and the locations of the revival patterns in the time interaction "domain" are independent of the intensities of the initial fields. Finally, observation of RCP has been performed using the one-atom mazer [2], which is more sophisticated than the dynamics of the JCM. Moreover, schemes for observing RCP via homodyne detection [17], photon counting experiment and homodyne tomography [6] have been reported.

Recently we have developed a new technique showing how within the single-mode multiphoton JCM the RCP of the atomic inversion of the single-photon JCM [17] and two-photon JCM [18] can be manifested in the evolution of the quadrature squeezing of the radiation field. Also the technique has been applied to two-mode single-photon JCM [19] and to higher-order squeezing [20]. The technique is based on two approaches: natural and numerical-simulation approaches. For the former there is a class of states whose squeezing factors can directly include information on the corresponding atomic inversion, however, for the latter the evolution of the quadrature squeezing of the three-photon JCM reflects the RCP involved in the $\langle\hat{\sigma}_z(T)\rangle$ of the single-photon JCM for the same initial field state. In this paper we apply this technique for the multiphoton IJCM. For such system we derive the rescaled squeezing factor, which can give information on the atomic inversion of the standard, i.e. single-photon transition, IJCM. Also we discuss the required condition for obtaining best information from the quadrature squeezing about the atomic inversion and investigate the influence of the detuning parameter on such relation. Moreover, we investigate these two issues for the standard JCM (SJCM) since they have not been discussed yet. These results and those in [17, 18, 20] show that the RCP occurred in $\langle\hat{\sigma}_z(T)\rangle$ can be detected using techniques similar to those used for quadrature squeezing, e.g. homodyne detector [22], nonlinear homodyne detector [23] and multiport homodyne detector [24]. It is worth mentioning that in cavity QED, the homodyne detector technique has been applied to the single Rydberg atom and one-photon field for studying the field phase evolution of the regular JCM [25]. The final remark the generation of nonclassical squeezed light in the IJCM has been reported in [21].

The paper is prepared in the following order. In section 2 we give the basic relations and

equations including the Hamiltonian model, the definition of quadrature squeezing and discuss the influence of the detuning parameter on the evolution of the $\langle\hat{\sigma}_z(T)\rangle$. In sections 3 and 4 we investigate the occurrence of RCP in the squeezing factors for the resonance and off-resonance cases, respectively. In section 5 the main conclusions are summarized.

II. BASIC RELATIONS AND EQUATIONS

In this section we give the basic relations and equations, which mainly be used in the paper. Precisely, we write down the Hamiltonian model of the system, its wave function and the definition of quadrature squeezing. Additionally we shed briefly the light on the influence of detuning parameter on the evolution of the atomic inversion.

The Hamiltonian controlling the IJCM in the rotating wave approximation is [26]:

$$\frac{\hat{H}}{\hbar} = \omega\hat{a}^{\dagger}\hat{a} + \frac{1}{2}\omega_a\hat{\sigma}_z + \lambda(\hat{R}\hat{\sigma}_+ + \hat{R}^{\dagger}\hat{\sigma}_-), \tag{1}$$

where

$$\hat{R} = \hat{a}^m f(\hat{n}), \qquad \hat{n} = \hat{a}^{\dagger}\hat{a} \tag{2}$$

and $f(.)$ is a function in the mean-photon number, which is restricted to $f(\hat{n}) = \sqrt{\hat{n}}$ for IJCM and $f(.) = 1$ for SJCM. Also $\hat{\sigma}_{\pm}$ and $\hat{\sigma}_z$ are the Pauli spin operators; ω and ω_a are the frequencies of the cavity mode $\hat{a}$ and the atom, respectively; λ is the atom-field coupling constant and m is the transition parameter.

For obtaining the dynamical state of (1) we define two operators $\hat{F}_1$ and $\hat{F}_2$ as

$$\hat{F}_1 = \omega(\hat{a}^{\dagger}\hat{a} + \frac{m}{2}\hat{\sigma}_z), \qquad \hat{F}_2 = \frac{\Delta}{2}\hat{\sigma}_z + \lambda(\hat{R}\hat{\sigma}_+ + \hat{R}^{\dagger}\hat{\sigma}_-), \tag{3}$$

where $\Delta = \omega_a - m\omega$ is the detuning parameter. It is easy to prove that $\hat{F}_1$ and $\hat{F}_2$ are constants of motion. Basically, we consider the field and atom are initially prepared in coherent $|\alpha\rangle$ and excited atomic $|+\rangle$ states, respectively. In the interaction picture the dynamical state of the system can be evaluated as:

$$\begin{aligned} |\psi(T)\rangle &= \exp(-it\hat{F}_2)|+,\alpha\rangle \\ &= \sum_{n=0}^{\infty} C_n \left[G_1(n,m,T)|+,n\rangle + G_2(n,m,T)|-,n+m\rangle\right], \end{aligned} \tag{4}$$

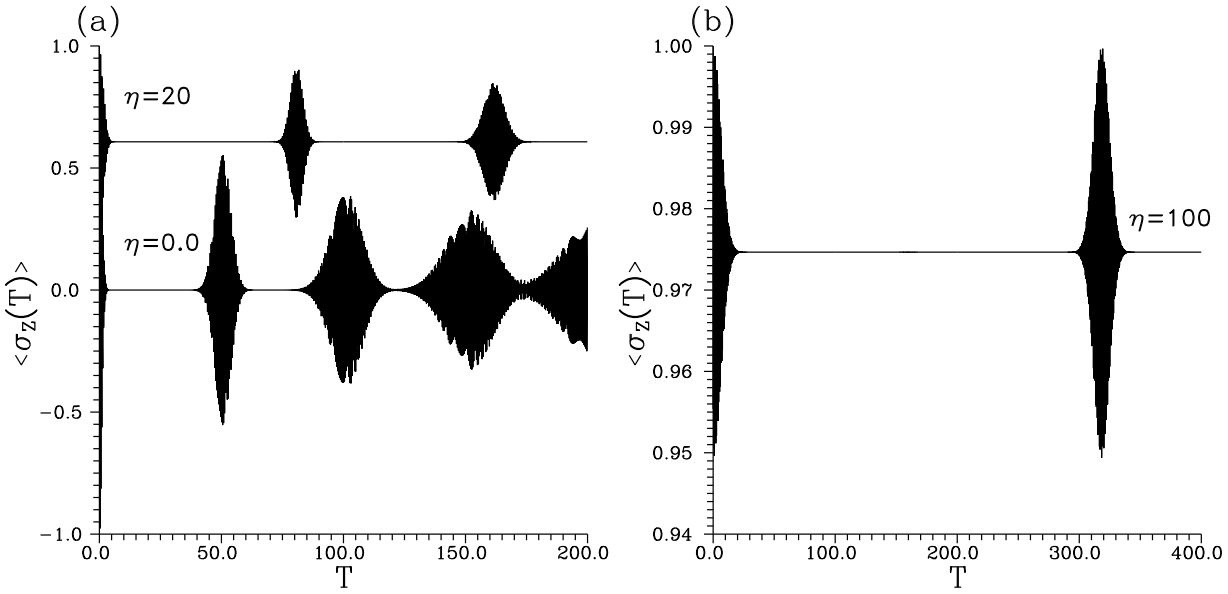

FIG. 1: The atomic inversion $\langle\hat{\sigma}_z(T)\rangle$ against the scaled time T for the SJCM when the cavity mode is initially prepared in the coherent state with $(\alpha, m) = (8, 1)$ and $\eta = 0, 20$ (a) and 100 (b).

where

$$T = \lambda t, \quad \eta = \frac{\Delta}{\lambda}, \qquad C_n = \exp(-\tfrac{1}{2}|\alpha|^2)\frac{\alpha^n}{\sqrt{n!}}, \qquad \gamma_{n,m} = \sqrt{\frac{\eta^2}{4} + \frac{(n+m)!}{n!}f^2(n+m)},$$

$$G_1(n, m, T) = \cos(T\gamma_{n,m}) - i\frac{\eta}{2\gamma_{n,m}}\sin(T\gamma_{n,m}), \tag{5}$$

$$G_2(n, m, T) = -i\sqrt{\frac{(n+m)!}{n!}}f(n+m)\frac{\sin(T\gamma_{n,m})}{\gamma_{n,m}}$$

and $|-\rangle$ denotes ground atomic state. Throughout the paper we consider α to be real. The atomic inversion related to (4) is

$$\langle\hat{\sigma}_z(T)\rangle = \sum_{n=0}^{\infty} P(n)\Big[\frac{\frac{\eta^2}{4}}{\gamma_{n,m}^2} + \frac{\frac{(n+m)!}{n!}f^2(n+m)}{\gamma_{n,m}^2}\cos(2T\gamma_{n,m})\Big], \tag{6}$$

where $P(n) = |C_n|^2$. Information about (6) is shown in Figs. 1 and 2 for the SJCM and IJCM, respectively, for $m = 1$ and given values of the interaction parameters. From Figs. 1 one can observe that as the value of the detuning parameter η increases the collapse period and the width of the revival pattern increase. Moreover, when the detuning is very strong the atomic trapping occurs, which is close to its initial atomic state. This does not mean that the system stays in its initial state where the IJCM provides nonclassical squeezing for strong detuning [21]. Also such type of the atomic trapping is quite different from that occurring via controlling the values of the atomic relative phases [27] in which $\langle\hat{\sigma}_z(T)\rangle \simeq 0$. From Figs. 2, i.e. for IJCM, the RCP is

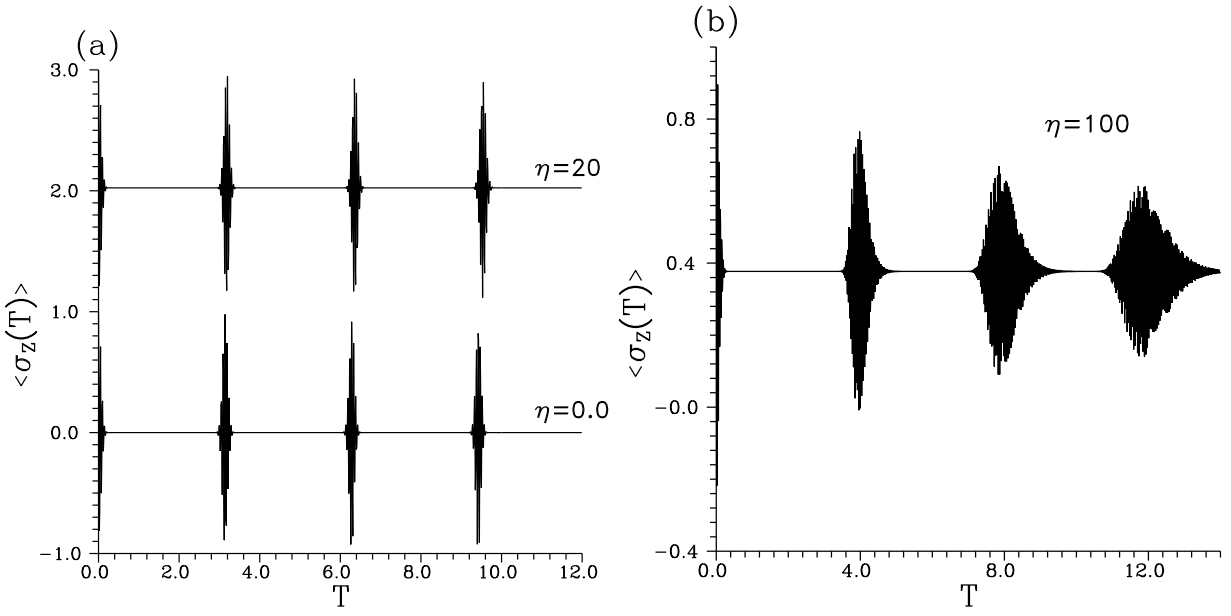

FIG. 2: The atomic inversion $\langle\hat{\sigma}_z(T)\rangle$ against the scaled time T for the IJCM when the cavity mode is initially prepared in the coherent state with $(\alpha, m) = (8, 1)$ and $\eta = 0, 20$ (a) and 100 (b).

remarkable, where for $\eta = 0$ the revival patterns are compact and occur periodically with period π. This behavior is dominant when the values of η and $\bar{n} = \langle\hat{n}(0)\rangle$ are comparable (compare the curves in Fig. 2(a)). For very strong value of η the RCP are established having features different from those for $\eta = 0$ in the sense that the revival patterns (collapse time) become broader (greater) than those of $\eta = 0$. Comparison between Figs. 1(b) and 2(b) shows that the atomic inversion of the IJCM goes to trapped atomic state in a rate slower than that of the SJCM. These facts can be partially realized from (6). In this equation when η is very strong and $\eta >> \bar{n}$ one can asymptotically consider $\frac{\eta^2}{\gamma^2_{n,m}} \simeq 1$ (i.e., the first summation tends to unity) and $\frac{\frac{(n+m)!}{n!} f^2(n+m)}{\gamma^2_{n,m}} \leq 1$ (i.e., the absolute value of the second summation is less than 1 or it is close to zero). Leading that the overall behavior is close to unity. Furthermore, when $f(.) = \sqrt{\hat{n}}$ these coefficients tend to the specified values in rates slower than those of the case $f(.) = 1$. Thus the behavior associated with the IJCM is more stable than that of the SJCM. The sensitivity of the revival time to η can be analytically deduced. For instance, for the standard IJCM with the radiation field prepared initially in coherent light the revivals occur in the $\langle\hat{\sigma}_z(T)\rangle$ when neighbor terms in the sums are in phase. This can be expressed as:

$$
\begin{aligned}
&2T_r \left[\sqrt{(\tfrac{\eta}{2})^2 + (\langle\hat{n}(0)\rangle + 1)^2} - \sqrt{(\tfrac{\eta}{2})^2 + \langle\hat{n}(0)\rangle^2}\right] \simeq 2\pi, \\
&T_r \left\{\sqrt{(\tfrac{\eta}{2})^2 + \langle\hat{n}(0)\rangle^2}\left[1 + \tfrac{2\langle\hat{n}(0)\rangle+1}{2(\frac{\eta}{2})^2+2\langle\hat{n}(0)\rangle^2}\right] - \sqrt{(\tfrac{\eta}{2})^2 + \langle\hat{n}(0)\rangle^2}\right\} \simeq \pi,
\end{aligned}
\tag{7}
$$

where T_r denotes the revival time associated with the IJCM. When $\langle\hat{n}(0)\rangle$ is large we can consider $2\langle\hat{n}(0)\rangle + 1 \simeq 2\langle\hat{n}(0)\rangle$. Consequently expression (7) reduces to

$$T_r \simeq \frac{\pi\sqrt{(\frac{\eta}{2})^2 + \langle\hat{n}(0)\rangle^2}}{\langle\hat{n}(0)\rangle}. \tag{8}$$

It is evident that when $\eta = 0$ expression (8) reduces to that of the resonance case, i.e. $T_r = \pi$. Similar procedures for SJCM with $m = 1$ provide the revival time T_r' as

$$T_r' \simeq 2\pi\sqrt{(\frac{\eta}{2})^2 + \langle\hat{n}(0)\rangle}. \tag{9}$$

The validity of (9) and (8) can be checked for the first revivals of $\eta = 20, 100$ in Figs. 1 and 2. One can also realize that when $\eta \to \infty$ the revival times become infinity. These results agree with those given for the nonlinear JCM in [14].

Now–for the sake of convenience–we define two quadrature operators for Nth-order squeezing as $\hat{X}_N = \frac{1}{2}(\hat{a}^N + \hat{a}^{\dagger N}), \quad \hat{Y}_N = \frac{1}{2i}(\hat{a}^N - \hat{a}^{\dagger N})$, where N is a positive integer. These quadratures satisfy the commutation rule $[\hat{X}, \hat{Y}] = \frac{i\hat{C}_N}{2}$, where $\hat{C}_N = \hat{a}^N\hat{a}^{\dagger N} - \hat{a}^{\dagger N}\hat{a}^N$. Thus the uncertainty relation is $\langle(\triangle\hat{X}(T))^2\rangle\langle(\triangle\hat{Y}(T))^2\rangle \geq \frac{|\langle\hat{C}_N\rangle|^2}{16}$. The squeezing factors associated with $\hat{X}_N$ and $\hat{Y}_N$ can be respectively expressed as [28]:

$$\begin{aligned} S_N(T) &= \langle\hat{a}^{\dagger N}(T)\hat{a}^N(T)\rangle + \mathrm{Re}\langle\hat{a}^{2N}(T)\rangle - 2(\mathrm{Re}\langle\hat{a}^N(T)\rangle)^2, \\ Q_N(T) &= \langle\hat{a}^{\dagger N}(T)\hat{a}^N(T)\rangle - \mathrm{Re}\langle\hat{a}^{2N}(T)\rangle - 2(\mathrm{Im}\langle\hat{a}^N(T)\rangle)^2. \end{aligned} \tag{10}$$

Here we shed briefly the light on the natural approach for the IJCM since it is similar to that of the SJCM [17]. In this approach the squeezing factors provide direct information on the atomic inversion. This is based on the fact that $\hat{F}_1$ is a constant of motion, i.e. the quantities $\langle\hat{\sigma}_z(T)\rangle$ and $\langle\hat{a}^\dagger(T)\hat{a}(T)\rangle$ carry information on each other. This approach is established for particular type of initial states of the radiation field, which verify, e.g. for $N = 1$ normal squeezing, the conditions

$$\langle\hat{a}(T)\rangle = 0, \qquad \langle\hat{a}^2(T)\rangle = 0 \tag{11}$$

simultaneously. This can occur when the mode is initially prepared in three-photon states [29], four-photon states [30],.. etc. In this case, similar to the SJCM [20], one can easily prove that

$$\langle\hat{\sigma}_z(T)\rangle = 2\langle\hat{a}^\dagger(0)\hat{a}(0)\rangle + 1 - 2S_1(T). \tag{12}$$

Expression (12) shows that the atomic inversion can be readout from the quadrature squeezing. We have to stress that the expression (12) is the same for resonance and off-resonance cases. Moreover, expression of the higher-order squeezing for IJCM can be also derived similar to that in [17].

In the following sections we use the relations given in the present section to investigate numerically how within the multiphoton IJCM the quadratures squeezing exhibit the RCP similar to that involved in the evolution of the atomic inversion of the standard IJCM with initial coherent light. We discuss to which value of the initial mean-photon number the quadrature squeezing gives the most appropriate information on the atomic inversion. Also we investigate the influence of the detuning parameter on the under consideration phenomenon for SJCM and IJCM.

III. RESONANCE CASE

In this section we investigate the possibility to obtain RCP from the second-order quadrature squeezing of the mth-photon ($m > 1$) IJCM for $\eta = 0$ similar to that of the standard IJCM (, i.e. $\langle\hat{\sigma}_z(T)\rangle_{m=1}$) when the field is initially in the coherent state. According to the line given in [17] the RCP can occur only in $Q_1(T)$ and the quantity $\mathrm{Re}\langle\hat{a}^2(T)\rangle$ is responsible for such behavior. Thus we give a closer look at the expression of the $\langle\hat{a}^2(T)\rangle$, which from (4) can be evaluated as:

$$\langle\hat{a}^2(T)\rangle = \alpha^2 \sum_{n=0}^{\infty} P(n)\Big\{\cos(T\gamma_{n+2,m})\cos(T\gamma_{n,m}) + \sqrt{\tfrac{(n+m+1)(n+m+2)}{(n+1)(n+2)}}\sin(T\gamma_{n+2,m})\sin(T\gamma_{n,m})\Big\}. \tag{13}$$

In the strong-intensity regime, i.e. $\bar{n} = |\alpha|^2 >> 1$, and finite values of the transition parameter m, we can apply the harmonic approximation technique [12]: for Poissonian photon-number distribution such as that of the coherent light the terms contributing effectively to the summation in (13) are those for which $n \simeq \bar{n}$. Consequently the square root in the second line of (13) tends to unity and (13) reduces to

$$\langle\hat{a}^2(T)\rangle \simeq \bar{n}\sum_{n=0}^{\infty} P(n)\cos[T(\gamma_{n+2,m} - \gamma_{n,m})]. \tag{14}$$

Comparison between (6) (for $\eta = 0$ and $m = 1$) and (14) shows that the two expressions can exhibit similar dynamical behavior only when the arguments of cosines in the two expressions are comparable. Therefore, we seek the proportionality factor μ_1, say, which can play this role. This

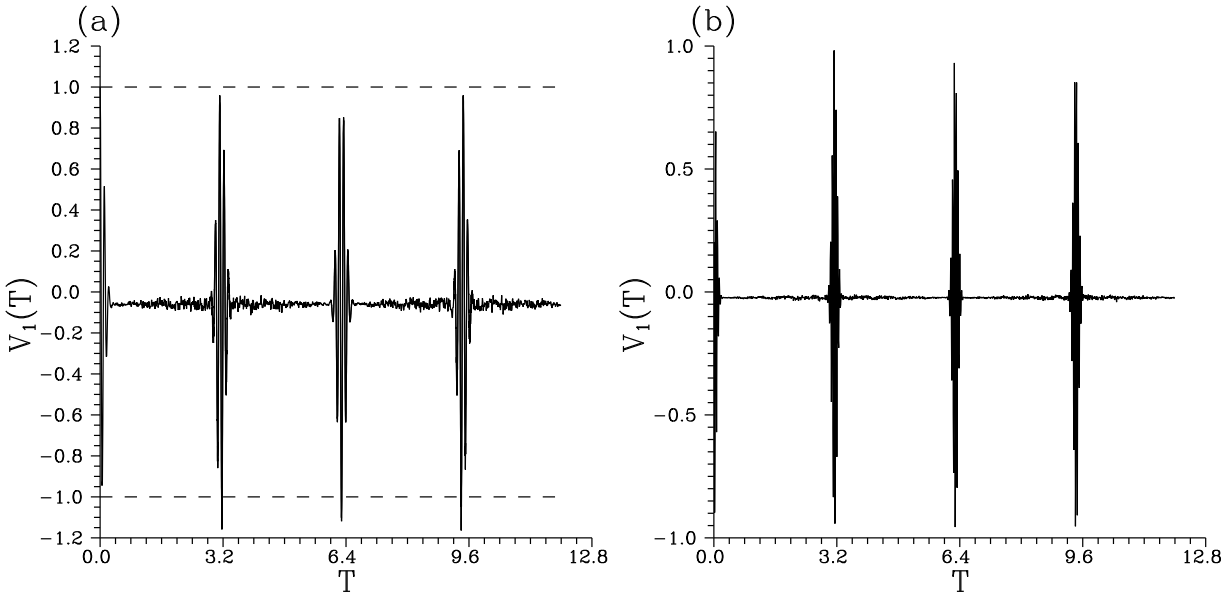

FIG. 3: The rescaled squeezing factor $V_1(T)$ for the IJCM when $m = 3$, $\alpha = 5$ (a) and 8 (b).

factor can be evaluated from the following expression:

$$\mu_1 = \frac{\gamma_{n+2,m} - \gamma_{n,m}}{2(n+1)}. \tag{15}$$

Expression (15) can be re-expressed as

$$\mu_1 = \tfrac{1}{2(n+1)}\sqrt{\tfrac{(n+m)!}{(n+2)!}}\Big\{\sqrt{(n+m+2)^2(n+m+1)} - \sqrt{(n+m)(n+1)(n+2)}\Big\}$$

$$= \frac{n^{\frac{m-7}{2}}}{2(1+\frac{1}{n})\sqrt{(1+\frac{1}{n})(1+\frac{2}{n})}}\left[\prod_{j=0}^{m}(1+\tfrac{m-j}{n})\right]^{\frac{1}{2}} \tag{16}$$

$$\times\frac{\left[2n^2(m+1)+(3m^2+7m+6)n+(m+2)^2(1+m)-2m\right]}{[(1+\frac{m+2}{n})\sqrt{1+\frac{m+1}{n}}+\sqrt{(1+\frac{m}{n})(1+\frac{1}{n})(1+\frac{2}{n})}]}.$$

In the strong-intensity regime, where the harmonic approximation can be applied (, i.e. $\epsilon/n \to 0$, where ϵ is an arbitrary finite number) the equation (16) reduces to

$$\mu_1 \simeq \frac{1}{4}\Big\{2(m+1)\bar{n}^{\frac{m-3}{2}} + (3m^2+7m+6)\bar{n}^{\frac{m-5}{2}} + [(m+2)^2(1+m)-2m]\bar{n}^{\frac{m-7}{2}}\Big\}. \tag{17}$$

From (17) the RCP can occur in the evolution of the $Q_1(T)$ only when $m = 3$, which is similar to that of SJCM [17]. In this case the proportionality factor is $\mu_1 = 2$. Furthermore, one can use the same procedures (for complete details the reader can consult [18, 20]) for evaluating the proportionality factor of the Nth-order squeezing, which is $\mu_1 = 2N$. For the sake of generalization we write down the Nth-order rescaled squeezing factor as

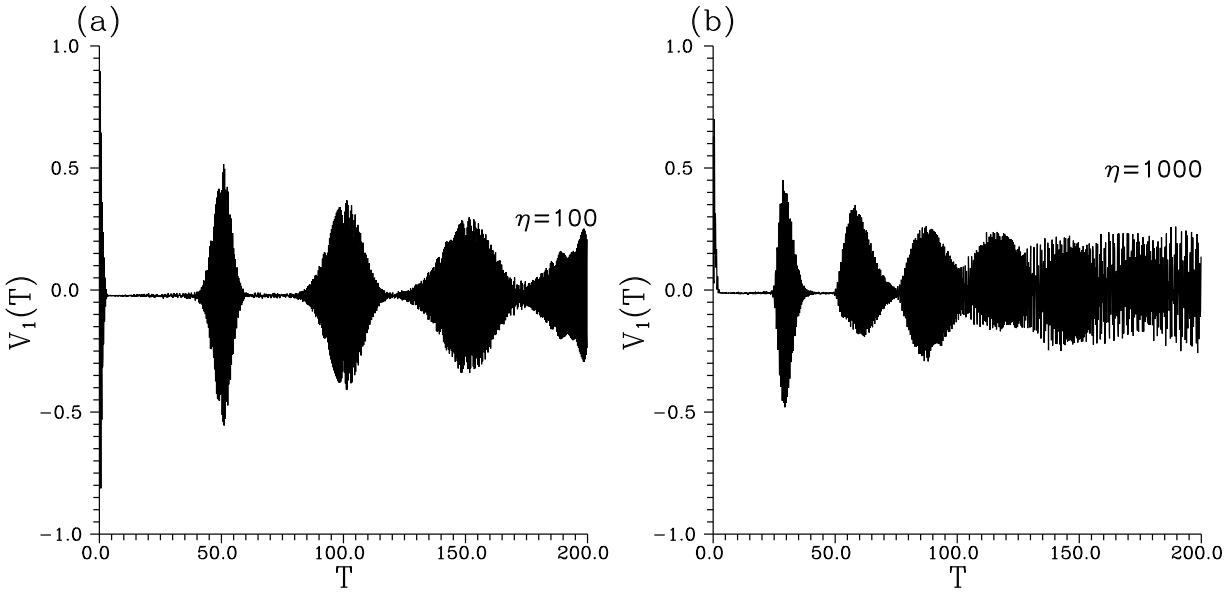

FIG. 4: The rescaled squeezing factor $V_1(T)$ for the SJCM when $(\alpha, m) = (8, 3)$, $\eta = 100$ (a) and 1000 (b).

$$V_N(T) = \frac{\langle \hat{n}(0) \rangle^N - Q(\frac{bT}{N})}{\langle \hat{n}(0) \rangle^N}, \tag{18}$$

where the parameter b takes on 2/3 for $f(.) = 1$ [17, 20] and 1/2 for $f(.) = \sqrt{\hat{n}}$, which is the case under consideration. For normal squeezing and $f(.) = \sqrt{\hat{n}}$ we have plotted $V_1(T)$ for $\alpha = 5$ (a) and $\alpha = 8$ (b) against the scaled time T in Figs. 3(a) and (b), respectively. Comparison between the curve associated with $\eta = 0$ in Fig. 2(a) with those presented in Figs. 3 demonstrate our conclusion: the rescaled squeezing factor (18) can give information on the atomic inversion of the standard IJCM. On the other hand, we can see that both curves in Figs. 3 provide information on the atomic inversion, however, Fig. 3(b) exhibits better information than that of the Fig. 3(a) (compare the shape of the collapse regions and the amplitude of the revival patterns). This leads to the following question: which values of the initial mean-photon number can give perfect information on the atomic inversion? The answer for this question can be easily realized, e.g. for normal squeezing, from (17). More precisely, the technique works well when the value of the second term in the rectangular brackets is close to zero. This can be expressed as:

$$(3m^2 + 7m + 6)\bar{n}^{\frac{m-5}{2}} < 1. \tag{19}$$

For $m = 3$ the inequality (19) reduces to $\bar{n} > 54$. This agrees with the information shown in Figs. 3. As the value of the squeezing-order N increases the value of the initial mean-photon

number required for giving better information on $\langle\hat{\sigma}_z(T)\rangle_{m=1}$ has to be increased, e.g. for the amplitude-squared squeezing we have to use $\langle\hat{n}(0)\rangle > 226$ (we have checked this fact). On the other hand, for SJCM, i.e. $f(.) = 1$, the $\langle\hat{n}(0)\rangle > 18$ and 144 for the normal and amplitude-squared squeezing, respectively. In conclusion, for strong initial mean-photon number the formula (18) works regardless of the condition (19) where the overall behaviors of the rescaled squeezing factor and atomic inversion are similar. Hoever, to obtain typical information from these two quantities such type of condition has to be fulfilled.

IV. OFF-RESONANCE CASE

In this section we discuss the off-resonance case $\eta \neq 0$ for the multiphoton SJCM and IJCM in the framework of the numerical approach. It is worth reminding that the $\langle\hat{\sigma}_z(T)\rangle$ is sensitive to the value of the detuning parameter. We restrict the discussion to the normal squeezing, where the higher-order squeezing can be similarly understood. There are some facts we would like to address here. For $\eta \neq 0$ we have $\mathrm{Re}\langle\hat{a}(T)\rangle \neq 0$ and $\mathrm{Im}\langle\hat{a}(T)\rangle \neq 0$, which likely indicates that the technique does not work correctly. Nevertheless, we have noted that the values of $\mathrm{Im}\langle\hat{a}(T)\rangle$ are considerably small compared to the other terms in the squeezing factor. This means that if the squeezing factors exhibit information about $\langle\hat{\sigma}_z(T)\rangle$ this probably occur in $Q_1(T)$. In this case the quantity $\mathrm{Re}\langle\hat{a}^2(T)\rangle$ is responsible for this. This behavior is typical to that of the resonance case (cf. section 3). As there is a difficulty to derive the rescaled squeezing factor for $\eta \neq 0$ we investigate the influence of η on the formula (18). We have noted that this formula for $\eta \neq 0$ provides RCP typical to that of $\eta = 0$, however, for very strong values of η the RCP is different from that of the $\langle\hat{\sigma}_z(T)\rangle_{m=1}$. These facts are shown in Figs. 4 and 5 for given values of the parameters. For SJCM comparison between Figs. 1(a), 1(b) and Fig. 4(a) demonstrate the main conclusion. From Fig. 4(b) where η is very strong the revival patterns are increased, blurred and overlapped for large time interaction. This is in contrast with the corresponding case of the $\langle\hat{\sigma}_z(T)\rangle_{m=1}$. Similar remarks may be quoted for IJCM (see Figs. 5). Additionally, the RCP involved in (18) for IJCM is much stable than that for SJCM, i.e. it needs values of η greater than those for SJCM to be deviated from that of the atomic inversion.

Now we partially explain the results shown in Figs. 4 and 5 as follows. The quantity $\mathrm{Re}\langle\hat{a}^2(T)\rangle$ plays the essential role in the behavior of the rescaled squeezing factor, which can be evaluated for

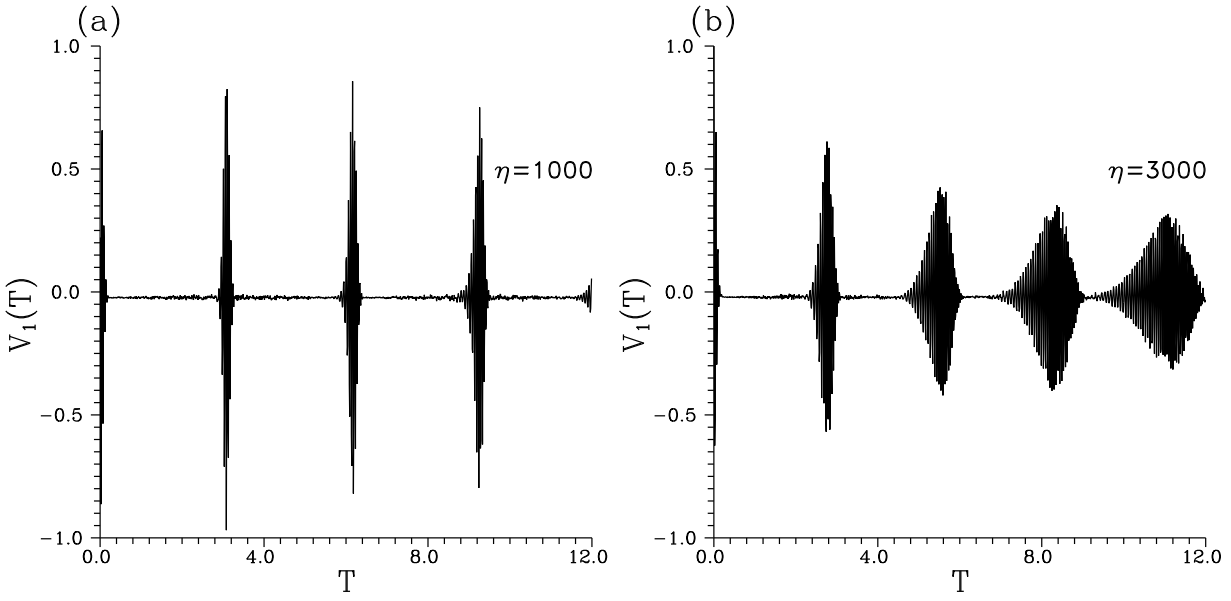

FIG. 5: The rescaled squeezing factor $V_1(T)$ for the IJCM when $(\alpha, m) = (8, 3)$, $\eta = 1000$ (a) and 3000 (b).

the state (4) as:

$$\mathrm{Re}\langle\hat{a}^2(T)\rangle = \alpha^2 \sum_{n=0}^{\infty} P(n)\Big\{\cos(T\gamma_{n+2,m})\cos(T\gamma_{n,m}) + \left[\frac{\frac{\eta^2}{4}+\frac{(n+m+2)!}{(n+2)!}f(n+m)f(n+m+2)}{\gamma_{n+2,m}\gamma_{n,m}}\right]\sin(T\gamma_{n+2,m})\sin(T\gamma_{n,m})\Big\}. \tag{20}$$

In the strong-intensity regime and finite value of m the rectangular brackets in the second line of (20) tends to unity and we arrive at

$$\mathrm{Re}\langle\hat{a}^2(T)\rangle = \alpha^2 \sum_{n=0}^{\infty} P(n)\cos(T\Omega_n), \tag{21}$$

where the generalized Rabi frequency Ω_n takes the form

$$\Omega_n = \sqrt{\frac{\eta^2}{4} + \frac{(n+m+2)!}{(n+2)!}f^2(n+m+2)} - \sqrt{\frac{\eta^2}{4} + \frac{(n+m)!}{n!}f^2(n+m)}. \tag{22}$$

The behavior of the $V_1(T)$ is a direct consequence form the "evolution" of the generalized Rabi frequency Ω_n in the range of n for which $P(n)$ has an effective contribution. Therefore, for IJCM we plot Ω_n and $P(n)$ against n in Fig. 6 for values of parameters as those given for Figs. 5. For the sake of comparison between these two quantities we rescaled Ω_n by 1/6000. From this figure one can observe that for $\eta = 0$ the generalized Rabi frequency Ω_n is linear, i.e. straightline curve, however, when $\eta \neq 0$ nonlinearity occurs (see short-dashed and long-dashed curves). In all cases the curves are growing function of n. Most importantly, for $\eta = 1000$ the generalized Rabi frequency

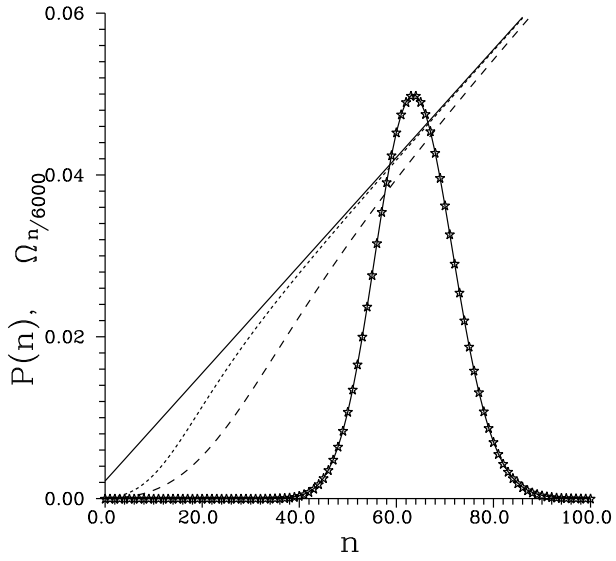

FIG. 6: The generalized Rabi frequency Ω_n and the photon-number distribution $P(n)$ (star-centered curve) against n for IJCM when $(\alpha, m) = (8, 3)$. For Ω_n solid, short-dashed and long-dashed curves are given respectively for $\eta = 0, 1000$ and 3000.

in the range of $P(n) \neq 0$ is almost equal to that of $\eta = 0$. This makes the behavior of $V_1(T)$ for these two cases are almost the same. Comparison between the short-dashed and long-dashed curves shows that when η is very large the deviation form the resonance case is established. This agrees with information shown in Figs. 5(a) and (b). Similar treatment can be given for SJCM.

V. CONCLUSIONS

In this paper we have discussed the possibility of including the squeezing factors of the multi-photon IJCM information on the atomic inversion of the standard IJCM. We have discussed the restriction on the values of the initial mean-photon number, which can give the most appropriate information about the atomic inversion. For the natural approach we have briefly shown that for particular type of initial states the squeezing factor for the off-resonance IJCM is similar to that of the resonance SJCM [17]. In this approach the squeezing factors provide complete information on the atomic inversion. For the resonance IJCM we have shown that the rescaled squeezing factor of the three-photon transition IJCM can give information on the atomic inversion of the standard IJCM. On the other hand, for the off-resonance IJCM and SJCM we have shown that the rescaled squeezing factor gives always $\langle \hat{\sigma}_z(T) \rangle_{m=1}$ of the $\Delta = 0$ for the finite values of the detuning parameter, however, for the large values of Δ it exhibits RCP different from that of the atomic inversion. We have explained such behavior by comparing the evolution of the generalized Rabi frequency for

different values of Δ.

References

[1] Jaynes E T and Cummings F W 1963 Proc. IEEE **51** 89.

[2] Rempe G, Walther H and Klein N 1987 *Phys. Rev. Lett.* **57** 353.

[3] El-Orany F A A and Obada A-S 2003 *J. Opt. B: Quant. Semiclass. Opt.* **5** 60, and references therein.

[4] Buck B and Sukumar C V 1981 *Phys. Lett. A* **81** 132; Sukumar C V and Buck B 1984 *J. Phys. A* **7** 877.

[5] Cardimona D A, Kovanis V, Sharma M P and Gavrielides A 1991 *Phys. Rev. A* **43** 3710, and references therein.

[6] Faisal A A El-Orany 2004 *J. Phys. A: Math. Gen.* **37** 6157.

[7] Faisal A A El-Orany, Mahran M H, Wahiddin M R B and Hashim A M 2004 *Opt. Commun.* **240** 169.

[8] Cardimona D A, Sharma M P and Ortega M A 1989 *J. Phys. B* **22** 4029; Cardimona D A 1990 *Phys. Rev. A* **41** 5016.

[9] Barnett S M and Knight P L 1984 *Opt. Acta* **31** 435; ibid 1203; Mahmood S and Zubairy M S 1987 *Phys. Rev. A* **35** 425; Iqbal M S, Mahmood S, Razmi M S K and Zubairy M S 1988 *Opt. Soc. Am. B* **5** 1312; Sharma M P, Cardimona D A and Gavrielides A 1989 *Opt. Commun.* **72** 291; Sharma M P, Cardimona D A and Gavrielides A 1989 *J. Opt. Soc. Am. B* **6** 1942.

[10] Kim M S 1993 *J. Mod. Opt.* **40** 1331.

[11] Meystre P and Zubairy M S 1982 *Phys. Lett. A* **89A** 390.

[12] Eberly J H, Narozhny N B and Sanchez-Mondragon J J 1980 *Phys. Rev. Lett.* **44** 1323; Narozhny N B, Sanchez-Mondragon J J and Eberly J H 1981 *Phys. Rev. A* **23** 236; Yoo H I, Sanchez-Mondragon J J and Eberly J H 1981 *J. Phys. A* **14** 1383; Yoo H I and Eberly J H 1981 *Phys. Rep.* **118** 239.

[13] Garraway B M, Sherman B, Moya-Cessa H, Knight P L and Kurizki G 1994 *Phys. Rev. A* **49** 535; Kozhekin A, Kurizki G and Sherman B 1996 *Phys. Rev. A* **54** 3535.

[14] Góra P and Jedrzejek C 1992 *Phys. Rev. A* **45** 6816.

[15] Satyanarayana M V, Rice P, Vyas R and Carmichael H J 1989 *J. Opt. Soc. Am. B* **6** 228.

[16] Alsingh P and Zubairy M S 1987 *J. Opt. Soc. Am. B* **4** 177; Puri R R and Bullough R K 1988 *J. Opt. Soc. Am. B* **5** 2021; Mahmood S and Ashraf M M 1996 *Opt. Commun.* **132** 457; Joshi A 2000 *Phys. Rev. A* **62** 043812.

[17] Faisal A A El-Orany 2004 *J. Phys. A: Math. Gen.* **37** 9023.

[18] Faisal A A El-Orany 2005 *Phys. Rev. A* (submitted).

[19] Faisal A A El-Orany 2005 *J. Opt. B: Quant. Semiclass. Opt.* (submitted).

[20] Faisal A A El-Orany 2004 *J. Phys. A: Math. Gen.* (at press).

[21] Bužek V 1989 *J. Mod. Opt.* **44** 675; Fu C.-R and Gong C.-D 1997 *J. Mod. Opt.* **44** 675.

[22] Mandel L and Wolf E 1995 "Optical Coherence and Quantum Optics" (Cambridge: University Press); Leonhardt U 1997 "Measuring the Quantum State of Light" (Cambridge: University Press).

[23] Wilkens M and Meystre P 1991 *Phys. Rev. A* **43** 3832.

[24] Walker N G 1987 *J. Mod. Opt.* **34** 15.

[25] Rauschenbeutel A, Nogues G, Osnaghi S, Bertet P, Brune M, Raimond J M and Haroche S 1999 *Phys. Rev. Lett.* **83** 5166; Bertet P, Auffeves A, Maioli P, Osnaghi S, Meunier T, Brune M, Raimond J M and Haroche S 2002 *Phys. Rev. Lett.* **89** 200402; Raimond J M, Brune M and Haroche S 2001 *Rev. Mod. Phys.* **73** 565.

[26] Rosenhouse-Dantsker A 1992 *J. Mod. Opt.* **39** 1471.

[27] Zaheer K and Zubairy M S 1989 *Phys. Rev. A* **39** 2000.

[28] Zhung Z-M, Xu L, Chui J-L, Li F-L 1990 *Phys. Lett. A* **150** 27.

[29] Braunstein S L and McLachlan R I 1987 *Phys. Rev. A* **45** 1659; Braunstein S L and Caves C M 1990 *Phys. Rev. A* **42** 4115.

[30] Lynch R 1994 *Phys. Rev. A* **49** 2800.